

Lepton flavour violation in rare Λ_b decays

MARZIA BORDONE,^a MUSLEM RAHIMI^b, K. KERI VOS^{c,d}

^a *Dipartimento di Fisica, Università di Torino & INFN, Sezione di Torino,
 I-10125 Torino, Italy*

^b *Center for Particle Physics Siegen (CPPS),
 Theoretische Physik 1, Universität Siegen,
 57068 Siegen, Germany*

^c *Gravitational Waves and Fundamental Physics (GWFP),
 Maastricht University, Duboisdomein 30,
 NL-6229 GT Maastricht, the Netherlands*

^d *Nikhef, Science Park 105,
 NL-1098 XG Amsterdam, the Netherlands*

Abstract

Lepton flavour violation (LFV) naturally occurs in many new physics models, specifically in those explaining the B anomalies. While LFV has already been studied for mesonic decays, it is important to consider also baryonic decays mediated by the same quark transition. In this paper, we present a first study of LFV in the baryonic $\Lambda_b \rightarrow \Lambda \ell_1 \ell_2$. We present expected bounds on the branching ratio in a model-independent framework and using two specific new physics models. Finally, we point out the interplay and orthogonality between the baryonic and mesonic LFV searches.

1 Introduction

The incredible joint theoretical and experimental effort carried out in the last years allows us to probe the Standard Model (SM) of particle physics with an unprecedented precision. This brought to light some deviations between theoretical predictions and experimental measurements in semileptonic B meson decays [1–15]. These discrepancies, the so-called B anomalies, hint at Lepton Flavour Universality (LFU) violation. This is quite surprising, as LFU is one of the foundation of the SM.

The B anomalies can be split into two classes: *i*) deviations in μ/e universality in $b \rightarrow s\ell^+\ell^-$ and *ii*) deviations in τ vs. light leptons universality in the $b \rightarrow c\ell\bar{\nu}$ transitions. These exciting findings may indicate the presence of New Physics (NP) particles, and have inspired a plethora of theoretical and experimental work. The NP explanations for B anomalies span a broad class of new heavy particles, from vectors to scalars states [16–57]. However, a common feature in all of these models is the prediction of sizeable effects for Lepton Flavour Violating (LFV) B , τ and μ decays. Current upper bounds on these modes largely constrain the allowed parameter space for NP models, and upcoming experimental analyses will be fundamental to corroborate or falsify these NP hypotheses.

When searching for LFV decays mediated by $b \rightarrow s\ell_1\ell_2$ transitions, it is crucial to consider both mesonic and baryonic decays. Although mediated by the same underlying partonic transition, these two types of decays provide orthogonal information on possible NP models. A striking example of this is the NP analysis of $\Lambda_b \rightarrow \Lambda\mu^+\mu^-$ decays [58], which shows that even though $B \rightarrow K\mu^+\mu^-$ angular distribution seems to be affected by some short-distance NP [59–62], the latter is not visible in the $\Lambda_b \rightarrow \Lambda\mu^+\mu^-$ angular observables. It is therefore natural to assume that $\Lambda_b \rightarrow \Lambda\ell_1^-\ell_2^+$ decays provide complementary information compared to their mesonic counterparts $B^+ \rightarrow K^+\ell_1\ell_2$ or $\bar{B}_s \rightarrow \ell_1\ell_2$ decays. In addition, the Λ_b baryon is copiously produced at LHCb and the dataset collected with Run 1 and Run 2 allow to make precision measurement of observables constructed from Λ_b decays (see e.g. [63]).

IN this paper, we calculate for the first time the angular distribution of $\Lambda_b \rightarrow \Lambda\ell_1^-\ell_2^+$ decays using a full base of NP operators (partial results are available in [64]). To achieve this, we use the decomposition of the $\Lambda_b \rightarrow \Lambda$ hadronic matrix elements in [65] and the lattice QCD determination of the corresponding form factors [66]. We then use model independent constraints to derive upper bounds for the branching ratio of $\Lambda_b \rightarrow \Lambda\ell_1^-\ell_2^+$ decays and specific models to provide predictions in a few scenarios [42, 43].

This paper is organised as follows: in Sect. 2 we highlight the main steps of our calculation and provide numerical results in a generic scenario. In Sect. 3 we use constraints on various LFV mesonic decays to put bounds on the branching ratio of $\Lambda_b \rightarrow \Lambda\ell_1^-\ell_2^+$, for different choices of leptons in the final state and make predictions for specific models. We conclude in Sect. 4.

2 The angular distribution of $\Lambda_b \rightarrow \Lambda \ell_1^- \ell_2^+$

In this Section, we introduce the concepts that we need for the study of phenomenological aspects in Sect. 3.

We consider the following effective Hamiltonian for LFV $b \rightarrow s \ell_1^- \ell_2^+$ transitions:

$$\mathcal{H}_{\text{eff}} = -\frac{4G_F}{\sqrt{2}} V_{tb} V_{ts}^* \frac{\alpha_{\text{em}}}{4\pi} \sum_{i=9,10,S,P} \left(C_i^{\ell_1 \ell_2}(\mu) \mathcal{O}_i^{\ell_1 \ell_2}(\mu) + C_i'^{\ell_1 \ell_2}(\mu) \mathcal{O}_i'^{\ell_1 \ell_2}(\mu) \right), \quad (1)$$

where the relevant operators are defined by

$$\begin{aligned} \mathcal{O}_9^{\ell_1 \ell_2} &= (\bar{s} \gamma_\mu P_L b) (\bar{\ell}_1 \gamma^\mu \ell_2), & \mathcal{O}_{10}^{\ell_1 \ell_2} &= (\bar{s} \gamma_\mu P_L b) (\bar{\ell}_1 \gamma^\mu \gamma^5 \ell_2), \\ \mathcal{O}_S^{\ell_1 \ell_2} &= (\bar{s} P_R b) (\bar{\ell}_1 \ell_2), & \mathcal{O}_P^{\ell_1 \ell_2} &= (\bar{s} P_R b) (\bar{\ell}_1 \gamma_5 \ell_2), \\ \mathcal{O}_T^{\ell_1 \ell_2} &= (\bar{s} \sigma^{\mu\nu} b) (\bar{\ell}_1 \sigma_{\mu\nu} \ell_2), & \mathcal{O}_{T5}^{\ell_1 \ell_2} &= (\bar{s} \sigma^{\mu\nu} b) (\bar{\ell}_1 \sigma_{\mu\nu} \gamma_5 \ell_2), \end{aligned} \quad (2)$$

and the operators with flipped chirality $\mathcal{O}_i'^{\ell_1 \ell_2}$ are obtained from $\mathcal{O}_i^{\ell_1 \ell_2}$ by replacing $P_L \leftrightarrow P_R$, where $P_{L/R} = \frac{1}{2}(1 \mp \gamma_5)$. Notice that the operator \mathcal{O}_7 :

$$\mathcal{O}_7 = \frac{m_b}{e} (\bar{s} \sigma_{\mu\nu} P_R b) F^{\mu\nu} \quad (3)$$

cannot generate LFV contributions due to the universality of electromagnetic interactions. In the following, we do not consider the operator $\mathcal{O}_{T(5)}^{\ell_1 \ell_2}$ as discussed in Sect. 3. We parametrise the hadronic matrix elements for $\Lambda_b(p, s_{\Lambda_b}) \rightarrow \Lambda(k, s_\Lambda)$ decays using an helicity decomposition [65–68]:

$$\begin{aligned} \langle \Lambda(k, s_\Lambda) | \bar{s} \gamma^\mu b | \Lambda_b(p, s_{\Lambda_b}) \rangle &= + \bar{u}_\Lambda(k, s_\Lambda) \left[f_0(q^2) (m_{\Lambda_b} - m_\Lambda) \frac{q^\mu}{q^2} \right. \\ &\quad + f_+(q^2) \frac{m_{\Lambda_b} + m_\Lambda}{s_+} \left(p^\mu + k^\mu - (m_{\Lambda_b}^2 - m_\Lambda^2) \frac{q^\mu}{q^2} \right) \\ &\quad \left. + f_\perp(q^2) \left(\gamma^\mu - \frac{2m_\Lambda}{s_+} p^\mu - \frac{2m_{\Lambda_b}}{s_+} k^\mu \right) \right] u_{\Lambda_b}(p, s_{\Lambda_b}), \end{aligned} \quad (4)$$

$$\begin{aligned} \langle \Lambda(k, s_\Lambda) | \bar{s} \gamma^\mu \gamma_5 b | \Lambda_b(p, s_{\Lambda_b}) \rangle &= - \bar{u}_\Lambda(k, s_\Lambda) \gamma_5 \left[g_0(q^2) (m_{\Lambda_b} + m_\Lambda) \frac{q^\mu}{q^2} \right. \\ &\quad + g_+(q^2) \frac{m_{\Lambda_b} - m_\Lambda}{s_-} \left(p^\mu + k^\mu - (m_{\Lambda_b}^2 - m_\Lambda^2) \frac{q^\mu}{q^2} \right) \\ &\quad \left. + g_\perp(q^2) \left(\gamma^\mu + \frac{2m_\Lambda}{s_-} p^\mu - \frac{2m_{\Lambda_b}}{s_-} k^\mu \right) \right] u_{\Lambda_b}(p, s_{\Lambda_b}), \end{aligned} \quad (5)$$

with $q = p - k$, $s_\pm = (m_{\Lambda_b} \pm m_\Lambda)^2 - q^2$, and s_{Λ_b} and s_Λ are the spin of the Λ_b and Λ baryons, respectively. Applying equations of motion to Eqs. (4)–(5), we obtain the following matrix

elements for scalar and pseudoscalar operators:

$$\langle \Lambda(k, s_\Lambda) | \bar{s} b | \Lambda_b(p, s_{\Lambda_b}) \rangle = \frac{m_{\Lambda_b} - m_\Lambda}{m_b(\mu) - m_s(\mu)} f_0 \bar{u}_\Lambda(k, s_\Lambda) u_{\Lambda_b}(p, s_{\Lambda_b}), \quad (6)$$

$$\langle \Lambda(k, s_\Lambda) | \bar{s} \gamma_5 b | \Lambda_b(p, s_{\Lambda_b}) \rangle = \frac{m_{\Lambda_b} + m_\Lambda}{m_b(\mu) + m_s(\mu)} g_0 \bar{u}_\Lambda(k, s_\Lambda) \gamma_5 u_{\Lambda_b}(p, s_{\Lambda_b}), \quad (7)$$

which agree with the expressions in Ref. [65]. In the following, we take the masses in $\overline{\text{MS}}$ using $\overline{m}_b(\overline{m}_b) = 4180 \text{ MeV}$ [69] and $\overline{m}_s(\overline{m}_b) = 78 \text{ MeV}$ [70].

2.1 Differential decay width and numerical analysis

We decompose the spin-independent double-differential decay width as

$$\frac{1}{\Gamma^{(0)}} \frac{d\Gamma(\Lambda_b(p, s_{\Lambda_b}) \rightarrow \Lambda(k, s_\Lambda) \ell_1^-(p_1) \ell_2^+(p_2))}{d \cos \theta_\ell dq^2} = a + b \cos \theta_\ell + c \cos^2 \theta_\ell, \quad (8)$$

with $\Gamma^{(0)} = \frac{\alpha_{\text{em}}^2 G_F^2 |V_{tb} V_{ts}^*|^2}{2048 \pi^5 m_{\Lambda_b}^3 q^2} \sqrt{\lambda_H} \sqrt{\lambda_L}$. We define $\lambda_H \equiv \lambda(m_{\Lambda_b}^2, m_\Lambda^2, q^2)$ and $\lambda_L \equiv \lambda(q^2, m_{\ell_1}^2, m_{\ell_2}^2)$, where λ is the usual Källén function defined as $\lambda(a, b, c) = a^2 + b^2 + c^2 - 2a(b+c) - 2bc$. Here $\cos \theta_\ell$ is the helicity angle in the dilepton frame as defined in Appendix A. The coefficients a , b and c are one of the main result of this work and have been calculated using the operator base in Eq. (1) and the decomposition for the hadronic matrix elements in Eqs. (4)–(5). We find:

$$\begin{aligned} a = & -\frac{1}{q^2} \left\{ |f_0|^2 \frac{(m_{\Lambda_b}^2 - m_\Lambda^2)^2}{q^2} s_+ [|C_{10+}^{\ell_1 \ell_2}|^2 (m_{\ell_1} + m_{\ell_2})^2 q_- + |C_{9+}^{\ell_1 \ell_2}|^2 (m_{\ell_1} - m_{\ell_2})^2 q_+] \right. \\ & + |f_\perp|^2 s_- [|C_{10+}^{\ell_1 \ell_2}|^2 (\lambda_L + 2q^2 q_+) + |C_{9+}^{\ell_1 \ell_2}|^2 (\lambda_L + 2q^2 q_-)] \\ & + |f_+|^2 (m_{\Lambda_b} + m_\Lambda)^2 s_- [|C_{10+}^{\ell_1 \ell_2}|^2 q_+ + |C_{9+}^{\ell_1 \ell_2}|^2 q_-] \\ & + |g_0|^2 \frac{(m_{\Lambda_b}^2 + m_\Lambda^2)^2}{q^2} s_- [|C_{10-}^{\ell_1 \ell_2}|^2 (m_{\ell_1} + m_{\ell_2})^2 q_- + |C_{9-}^{\ell_1 \ell_2}|^2 (m_{\ell_1} - m_{\ell_2})^2 q_+] \\ & + |g_\perp|^2 s_+ [|C_{10-}^{\ell_1 \ell_2}|^2 (\lambda_L + 2q^2 q_+) + |C_{9-}^{\ell_1 \ell_2}|^2 (\lambda_L + 2q^2 q_-)] \\ & \left. + |g_+|^2 (m_{\Lambda_b} - m_\Lambda)^2 s_+ [|C_{10-}^{\ell_1 \ell_2}|^2 q_+ + |C_{9-}^{\ell_1 \ell_2}|^2 q_-] \right\} \\ & - (q_- |C_{P-}^{\ell_1 \ell_2}|^2 + q_+ |C_{S-}^{\ell_1 \ell_2}|^2) \frac{s_- (m_{\Lambda_b} + m_\Lambda)^2}{(m_b + m_s)^2} |g_0|^2 - (q_- |C_{P+}^{\ell_1 \ell_2}|^2 + q_+ |C_{S+}^{\ell_1 \ell_2}|^2) \frac{s_+ (m_{\Lambda_b} - m_\Lambda)^2}{(m_b - m_s)^2} |f_0|^2 \\ & - \frac{2s_+}{q^2} \frac{(m_{\Lambda_b} - m_\Lambda)^2}{m_b - m_s} [\text{Re}(C_{10+}^{\ell_1 \ell_2} C_{P+}^{*\ell_1 \ell_2}) (m_{\ell_1} + m_{\ell_2}) q_- + \text{Re}(C_{9+}^{\ell_1 \ell_2} C_{S+}^{*\ell_1 \ell_2}) (m_{\ell_1} - m_{\ell_2}) q_+] |f_0|^2 \\ & - \frac{2s_-}{q^2} \frac{(m_{\Lambda_b} + m_\Lambda)^2}{m_b + m_s} [\text{Re}(C_{10-}^{\ell_1 \ell_2} C_{P-}^{*\ell_1 \ell_2}) (m_{\ell_1} + m_{\ell_2}) q_- + \text{Re}(C_{9-}^{\ell_1 \ell_2} C_{S-}^{*\ell_1 \ell_2}) (m_{\ell_1} - m_{\ell_2}) q_+] |g_0|^2, \end{aligned} \quad (9)$$

$$\begin{aligned}
b = & \frac{2}{q^4} [\text{Re}(f_0 f_+^*) (|C_{9+}^{\ell_1 \ell_2}|^2 + |C_{10+}^{\ell_1 \ell_2}|^2) + \text{Re}(g_0 g_+^*) (|C_{9-}^{\ell_1 \ell_2}|^2 + |C_{10-}^{\ell_1 \ell_2}|^2)] \sqrt{\lambda_H \lambda_L} (m_{\ell_2}^2 - m_{\ell_1}^2) (m_{\Lambda_b}^2 - m_{\Lambda}^2) \\
& - 4 [\text{Re}(C_{9-}^{\ell_1 \ell_2} C_{10+}^{*\ell_1 \ell_2}) + \text{Re}(C_{9+}^{\ell_1 \ell_2} C_{10-}^{*\ell_1 \ell_2})] \text{Re}(f_{\perp} g_{\perp}^*) \sqrt{\lambda_H \lambda_L} \\
& - \frac{2(m_{\Lambda_b}^2 - m_{\Lambda}^2)}{q^2(m_b - m_s)} \sqrt{\lambda_H \lambda_L} [\text{Re}(C_{10+}^{\ell_1 \ell_2} C_{P+}^{*\ell_1 \ell_2})(m_{\ell_1} - m_{\ell_2}) + \text{Re}(C_{9+}^{\ell_1 \ell_2} C_{S+}^{*\ell_1 \ell_2})(m_{\ell_1} + m_{\ell_2})] \text{Re}(f_0 f_+^*) \\
& - \frac{2(m_{\Lambda_b}^2 - m_{\Lambda}^2)}{q^2(m_b + m_s)} \sqrt{\lambda_H \lambda_L} [\text{Re}(C_{10-}^{\ell_1 \ell_2} C_{P-}^{*\ell_1 \ell_2})(m_{\ell_1} - m_{\ell_2}) + \text{Re}(C_{9-}^{\ell_1 \ell_2} C_{S-}^{*\ell_1 \ell_2})(m_{\ell_1} + m_{\ell_2})] \text{Re}(g_0 g_+^*),
\end{aligned} \tag{10}$$

$$\begin{aligned}
c = & + (|C_{9+}^{\ell_1 \ell_2}|^2 + |C_{10+}^{\ell_1 \ell_2}|^2) \frac{\lambda_L \lambda_H}{q^2 s_+} \left[-|f_+|^2 \frac{(m_{\Lambda_b} + m_{\Lambda})^2}{q^2} + |f_{\perp}|^2 \right] \\
& + (|C_{9-}^{\ell_1 \ell_2}|^2 + |C_{10-}^{\ell_1 \ell_2}|^2) \frac{\lambda_L \lambda_H}{q^2 s_-} \left[-|g_+|^2 \frac{(m_{\Lambda_b} - m_{\Lambda})^2}{q^2} + |g_{\perp}|^2 \right],
\end{aligned} \tag{11}$$

with $C_{X\pm}^{\ell_1 \ell_2} = (C_X^{\ell_1 \ell_2} \pm C_X'^{\ell_1 \ell_2})$ and $q_{\pm} = (m_{\ell_1} \pm m_{\ell_2})^2 - q^2$. Our results agree with [68] when setting $m_{\ell_1} = m_{\ell_2} = 0$. However, our convention for the helicity angle $\cos \theta_{\ell}$ has the opposite sign. Our formulae for the angular coefficients a, b, c also hold for $\Lambda_b \rightarrow \Lambda^* \ell_1^- \ell_2^+$ decays, when setting the additional perpendicular $\Lambda_b \rightarrow \Lambda^*$ form factor to zero. This is a reasonable approximation as in the Heavy-Quark-Expansion, this form factor is suppressed by Λ_{QCD}/m_b [71–73].

In the following, we focus on the branching ratio and forward-backward asymmetry:

$$\frac{d\mathcal{B}^{\ell_1 \ell_2}}{dq^2} = 2\Gamma^{(0)} \tau_{\Lambda_b} \left(a + \frac{c}{3} \right), \tag{12}$$

$$\frac{dA_{\text{FB}}^{\ell_1 \ell_2}}{dq^2} = \frac{\int_0^1 d\cos \theta \frac{d\Gamma}{d\cos \theta dq^2} - \int_{-1}^0 d\cos \theta \frac{d\Gamma}{d\cos \theta dq^2}}{\int_0^1 d\cos \theta \frac{d\Gamma}{d\cos \theta dq^2} + \int_{-1}^0 d\cos \theta \frac{d\Gamma}{d\cos \theta dq^2}} = \frac{b}{2(a + \frac{c}{3})}, \tag{13}$$

where the branching ratio $\mathcal{B} = \tau_{\Lambda_b} \Gamma$, where τ_{Λ_b} is the mean life of the Λ_b baryon [74] and Γ the total width. To evaluate the size of LFV $\Lambda_b \rightarrow \Lambda \ell_1^- \ell_2^+$ decay, we provide the q^2 -integrated quantities of Eqs. (12)–(13). For simplicity, we set $C_i'^{\ell_1 \ell_2} = 0$. Using the values for the masses from PDG [69], CKM factors from the UT-fit collaboration [75] and lattice QCD inputs for the form factors [66], we obtain

$$\begin{aligned}
10^8 \cdot \mathcal{B}^{\ell_1 \ell_2} = & \xi_9^{\ell_1 \ell_2} |C_9^{\ell_1 \ell_2}|^2 + \xi_{10}^{\ell_1 \ell_2} |C_{10}^{\ell_1 \ell_2}|^2 + \xi_S^{\ell_1 \ell_2} |C_S^{\ell_1 \ell_2}|^2 + \xi_P^{\ell_1 \ell_2} |C_P^{\ell_1 \ell_2}|^2 \\
& + \xi_{9S}^{\ell_1 \ell_2} \text{Re}(C_9^{\ell_1 \ell_2} C_S^{*\ell_1 \ell_2}) + \xi_{10P}^{\ell_1 \ell_2} \text{Re}(C_{10}^{\ell_1 \ell_2} C_P^{*\ell_1 \ell_2}),
\end{aligned} \tag{14}$$

$$\begin{aligned}
A_{\text{FB}}^{\ell_1 \ell_2} = & \left[\rho^{\ell_1 \ell_2} (|C_{10}^{\ell_1 \ell_2}|^2 + |C_9^{\ell_1 \ell_2}|^2) + \rho_{910}^{\ell_1 \ell_2} \text{Re}(C_9^{\ell_1 \ell_2} C_{10}^{*\ell_1 \ell_2}) \right. \\
& \left. + \rho_{9S}^{\ell_1 \ell_2} \text{Re}(C_9^{\ell_1 \ell_2} C_S^{*\ell_1 \ell_2}) + \rho_{10P}^{\ell_1 \ell_2} \text{Re}(C_{10}^{\ell_1 \ell_2} C_P^{*\ell_1 \ell_2}) \right] / \Gamma^{\ell_1 \ell_2},
\end{aligned} \tag{15}$$

	$\ell_1 = \mu, \ell_2 = \tau$	$\ell_1 = \mu, \ell_2 = e$
$\xi_9^{\ell_1 \ell_2}$	2.15 ± 0.11	3.13 ± 0.20
$\xi_{10}^{\ell_1 \ell_2}$	2.08 ± 0.10	3.13 ± 0.20
$\xi_S^{\ell_1 \ell_2}$	0.980 ± 0.057	1.83 ± 0.11
$\xi_P^{\ell_1 \ell_2}$	1.06 ± 0.06	1.83 ± 0.11
$\xi_{9S}^{\ell_1 \ell_2}$	-0.973 ± 0.059	0.142 ± 0.013
$\xi_{10P}^{\ell_1 \ell_2}$	1.20 ± 0.07	0.144 ± 0.013

Table 1: Numerical values for the parameters of Eq. (14). The coefficients do not depend on the charges of the final state leptons, except for $\xi_{9S}^{\ell_1 \ell_2}$ which changes sign when switching the charges of the leptons, i.e. $\xi_{9S}^{\tau\mu} = -\xi_{9S}^{\mu\tau}$ and $\xi_{9S}^{e\mu} = -\xi_{9S}^{\mu e}$. The uncertainties only include those from the form factor which are the dominant ones.

	$\ell_1 = \mu, \ell_2 = \tau$	$\ell_1 = \tau, \ell_2 = \mu$	$\ell_1 = \mu, \ell_2 = e$	$\ell_1 = e, \ell_2 = \mu$
$\rho^{\ell_1 \ell_2}$	1.26 ± 0.08	-1.26 ± 0.08	-0.025 ± 0.005	0.025 ± 0.005
$\rho_{910}^{\ell_1 \ell_2}$	-5.09 ± 0.24	-5.09 ± 0.24	-9.16 ± 0.55	-9.16 ± 0.55
$\rho_{9S}^{\ell_1 \ell_2}$	-2.23 ± 0.12	-2.23 ± 0.12	-0.283 ± 0.023	-0.283 ± 0.023
$\rho_{10P}^{\ell_1 \ell_2}$	1.99 ± 0.11	-1.96 ± 0.11	-0.280 ± 0.023	0.280 ± 0.023

Table 2: Coefficients for the numerator of $A_{\text{FB}}^{\ell_1 \ell_2}$. We give the values in units of $10^{-21} \text{ GeV}^{-1}$. This factor is compensated by the size of the decay width in Eq. (15).

with the numerical values for the coefficients $\xi_i^{\ell_1 \ell_2}$ and $\rho_i^{\ell_1 \ell_2}$ listed in Tables 1–2 and $\Gamma^{\ell_1 \ell_2}$ is the integrated width. We present only explicit results for the final states $\tau^\pm \mu^\mp$ and $\mu^\pm e^\mp$. The results for $\tau^\pm e^\mp$ can easily be obtained from the above results and agree within 1 σ with those of $\tau^\pm \mu^\mp$. The quoted uncertainties only include those from the form factors, which are the dominant ones. The correlation matrices between the two sets of $\{\xi_i^{\ell_1 \ell_2}, \rho_i^{\ell_1 \ell_2}\}$ coefficients are given in Appendix B. The $\xi_i^{\ell_1 \ell_2}$ coefficients in Table 1 do not depend on the charges of the final state leptons, except for $\xi_{9S}^{\ell_1 \ell_2}$ which depends on $(m_{\ell_1} - m_{\ell_2})$ and thus switches sign when switching the charges of the final state leptons, i.e. $\xi_{9S}^{\tau\mu} = -\xi_{9S}^{\mu\tau}$. Besides, we note that for μe final states, $\xi_9^{\ell_1 \ell_2} = \xi_{10}^{\ell_1 \ell_2}$ and $\xi_S^{\ell_1 \ell_2} = \xi_P^{\ell_1 \ell_2}$, such that only the combination $|C_9^{\ell_1 \ell_2}|^2 + |C_{10}^{\ell_1 \ell_2}|^2$ and $|C_P^{\ell_1 \ell_2}|^2 + |C_S^{\ell_1 \ell_2}|^2$ can be constrained. The coefficients $\rho_i^{\ell_1 \ell_2}$ in Table 2 are reported in units of $10^{-21} \text{ GeV}^{-1}$, which is then compensated in $A_{\text{FB}}^{\ell_1 \ell_2}$ by the size of the decay width.

3 Phenomenological implications

In the following, we discuss the implications of the available constraints on LFV B -meson decays and which bounds they imply on the observables in the baryonic modes. In order to do so, we need to choose which NP operators are present. Since no NP particles have been observed so far above the electroweak scale, we choose to work with the SMEFT:

$$\mathcal{L}_{\text{eff}} = \mathcal{L}_{\text{SM}} - \frac{1}{M^2} \left\{ [\mathcal{C}_{lq}^{(3)}]^{ij\alpha\beta} (\bar{Q}^i \gamma^\mu \sigma^a Q^j) (\bar{L}^\alpha \gamma_\mu \sigma^a L^\beta) + [\mathcal{C}_{lq}^{(1)}]^{ij\alpha\beta} (\bar{Q}^i \gamma^\mu Q^j) (\bar{L}^\alpha \gamma_\mu L^\beta) \right. \\ \left. + [\mathcal{C}_{ledq}]^{ij\alpha\beta} (\bar{Q}^i d_R^j) (\bar{e}_R^\alpha L^\beta) \right\}, \quad (16)$$

where we adopt the so-called Warsaw basis [76]. Here we denote with Q and L the left-handed quark and lepton doublets, respectively, and with e_R and d_R the right-handed charged leptons and down-type quarks, respectively. We further denote $\epsilon = i\sigma_2$ and M is the effective scale which can be associated with the mass of the heavy NP degrees of freedom.

The operators in Eq. (16) are the complete set of dimension-6 semileptonic operators that can contribute to $b \rightarrow s \ell_1 \ell_2$ transitions. We note that none of these operators contain a tensor current; nonetheless, at low energy, the operator $\mathcal{O}_{T(5)}^{\ell_1 \ell_2}$ defined in Eq. (2) could be generated through effective operators containing a covariant derivative [77]. However, as tensor operators provide a poor explanation for B anomalies (see e.g. [78]), we do not consider them in our analysis.

The Wilson coefficients of the operators in Eq. (16) can be constrained from low-energy processes as well as high- p_T data, and in general a flavour structure has to be assumed to reduce the number of independent NP parameters. In the following, we choose to consider only constraints from low-energy data and first do not to assume any hierarchy for the NP couplings. In Sect. 3.2 we then study particular scenarios, where a more complex structure for NP couplings in flavour space is assumed. For the $b \rightarrow s \ell_1 \ell_2$ transition we are interested in, we set $i = 2$ and $j = 3$ and generic $\alpha = \ell_1$ and $\beta = \ell_2$ in Eq. (16). Performing now the tree-level matching onto Eq. (1), we have

$$C_9^{\ell_1 \ell_2} = -C_{10}^{\ell_1 \ell_2} = + \frac{v^2}{\Lambda^2} \frac{\pi}{\alpha_{\text{em}} |V_{tb} V_{ts}^*|} \left([\mathcal{C}_{lq}^{(3)}]^{23\ell_1 \ell_2} + [\mathcal{C}_{lq}^{(1)}]^{23\ell_1 \ell_2} \right), \\ C_9^{\prime \ell_1 \ell_2} = +C_{10}^{\prime \ell_1 \ell_2} = + \frac{v^2}{\Lambda^2} \frac{\pi}{\alpha_{\text{em}} |V_{tb} V_{ts}^*|} [\mathcal{C}_{ld}]^{23\ell_1 \ell_2}, \\ C_S^{\ell_1 \ell_2} = -C_P^{\ell_1 \ell_2} = + \frac{v^2}{\Lambda^2} \frac{\pi}{\alpha_{\text{em}} |V_{tb} V_{ts}^*|} [\mathcal{C}_{ledq}]^{23\ell_1 \ell_2}, \\ C_S^{\prime \ell_1 \ell_2} = +C_P^{\prime \ell_1 \ell_2} = + \frac{v^2}{\Lambda^2} \frac{\pi}{\alpha_{\text{em}} |V_{tb} V_{ts}^*|} [\mathcal{C}_{ledq}^*]^{32\ell_1 \ell_2}. \quad (17)$$

Observable	Upper Bound
$\mathcal{B}(\bar{B}_s \rightarrow \mu^\pm \tau^\mp)$	$3.5 \cdot 10^{-5}$ [79]
$\mathcal{B}(\bar{B}_s \rightarrow \mu^\pm e^\mp)$	$5.4 \cdot 10^{-9}$ [80]
$\mathcal{B}(B^+ \rightarrow K^+ \tau^- \mu^+)$	$4.5 \cdot 10^{-5}$ [81]
$\mathcal{B}(B^+ \rightarrow K^+ \mu^- \tau^+)$	$3.9 \cdot 10^{-5}$ [82]
$\mathcal{B}(B^+ \rightarrow K^+ \mu^- e^+)$	$7.0 \cdot 10^{-9}$ [83]
$\mathcal{B}(B^+ \rightarrow K^+ e^- \mu^+)$	$6.4 \cdot 10^{-9}$ [83]

Table 3: Experimental upper limits for LFV B decays at 90% C.L..

	$\ell_1^- = \mu^-, \ell_2^+ = \tau^+$	$\ell_1^- = \mu^-, \ell_2^+ = e^+$
$c_{\ell_1 \ell_2}^{9+}$	1.09	1.75
$c_{\ell_1 \ell_2}^{10+}$	1.14	1.75
$c_{\ell_1 \ell_2}^S$	1.47	2.68
$c_{\ell_1 \ell_2}^P$	1.58	2.68
$c_{\ell_1 \ell_2}^{S9}$	-1.35	0.21
$c_{\ell_1 \ell_2}^{P10}$	1.66	0.21

Table 4: Predictions for the coefficients describing $B^+ \rightarrow K^+ \ell_1^- \ell_2^+$ decays using the hardonic form factors from Ref. [84,85]. We note that these coefficients are independent of the charges of the leptons, except for $c_{\ell_1 \ell_2}^{S9}$ which changes sign depending on the charge of the heavier lepton.

3.1 Model-independent approach

First, we consider the constraints on several combinations of Wilson coefficients from measurements of mesonic LFV decays. We consider the branching ratios of the decay modes $\bar{B}_s \rightarrow \ell_1^- \ell_2^+$ and $B \rightarrow K \ell_1^- \ell_2^+$, for which the experimental upper limits at 90% C.L. are reported in Table 4. Using Eq. (1), we have:

$$\begin{aligned}
\mathcal{B}(\bar{B}_s \rightarrow \ell_1^- \ell_2^+) &= \frac{\tau_{B_s}}{64\pi^3} \frac{\alpha_{\text{em}}^2 G_F^2 |V_{tb} V_{ts}^*|^2}{m_{B_s}^3} f_{B_s}^2 \lambda^{1/2}(m_{B_s}^2, m_1^2, m_2^2) \times \\
&\times \left\{ [m_{B_s}^2 - (m_1 - m_2)^2] \left| (m_1 + m_2) C_{10-}^{\ell_1 \ell_2} + \frac{m_{B_s}^2}{m_b + m_s} C_{P-}^{\ell_1 \ell_2} \right|^2 \right. \\
&\quad \left. + [m_{B_s}^2 - (m_1 + m_2)^2] \left| (m_1 - m_2) (C_{9-}^{\ell_1 \ell_2}) + \frac{m_{B_s}^2}{m_b + m_s} (C_{S-}^{\ell_1 \ell_2}) \right|^2 \right\}, \tag{18}
\end{aligned}$$

and

$$\begin{aligned} \mathcal{B}(B^+ \rightarrow K^+ \ell_1^- \ell_2^+) = 10^{-8} & \left\{ c_{\ell_1 \ell_2}^{9+} |C_{9+}^{\ell_1 \ell_2}|^2 + c_{\ell_1 \ell_2}^{10+} |C_{10+}^{\ell_1 \ell_2}|^2 + c_{\ell_1 \ell_2}^S |C_{S+}^{\ell_1 \ell_2}|^2 \right. \\ & \left. + c_{\ell_1 \ell_2}^P |C_{P+}^{\ell_1 \ell_2}|^2 + c_{\ell_1 \ell_2}^{S9} \text{Re}[C_{S+}^{*\ell_1 \ell_2} C_{9+}^{\ell_1 \ell_2}] + c_{\ell_1 \ell_2}^{P10} \text{Re}[C_{P+}^{*\ell_1 \ell_2} C_{10+}^{\ell_1 \ell_2}] \right\}, \end{aligned} \quad (19)$$

Both Eqs. (18)–(19) agree with previous results in the literature [86, 87]. Using again the values for the masses from PDG [69], CKM factors from the UT-fit collaboration [75], $f_{B_s} = 215 \text{ MeV}$ [88] and Lattice QCD/Light Cone Sum Rule results in Refs. [84, 85], we find the coefficients $c_{\ell_1 \ell_2}^i$ in Eq. (19) as listed in Table 4. Similar as for ξ_{9S} , the coefficient $c_{\ell_1 \ell_2}^{S9}$ is proportional to $m_1 - m_2$ and thus changes sign depending on charge of the heavier lepton. We stress that the numbers in Table 4 are strongly dependent on the choice for α_{em} . Here we take $\alpha_{\text{em}} = 1/133$. A different choice can be implemented by rescaling the $c_{\ell_1 \ell_2}^i$ coefficients.

Finally, we use the experimental upper bounds listed in Table 3 and Eqs. (18)–(19) to constrain different combinations of couplings $C_i^{\ell_1, \ell_2}$. As stated before, we do not consider τe decays as the constraints coming from these decays are similar to those from the $\tau \mu$ channel. Furthermore, for simplicity we also do not consider the $\mathcal{O}_i^{\prime \ell_1 \ell_2}$ operators. This choice is motivated by the fact that these operators are unappealing when trying to fit $b \rightarrow s \ell \ell$ data [59–62, 89]. Nevertheless, we stress that the baryonic channels have a different dependence on the primed operators with respect to the mesonic ones, which may be interesting to consider once scenarios involving these operators become more interesting to explain the B anomalies.

The obtained bounds for $\tau \mu$ and μe final states are given in Fig. 1 and in Fig. 2, respectively. We consider three 2-dimensional scenarios, in which we allow only some combinations of NP Wilson coefficients to be non-zero: $C_9^{\ell_1 \ell_2}$ and $C_{10}^{\ell_1 \ell_2}$, $C_S^{\ell_1 \ell_2}$ and $C_P^{\ell_1 \ell_2}$ and the SMEFT inspired one, where $C_9^{\ell_1 \ell_2} = -C_{10}^{\ell_1 \ell_2}$ and $C_S^{\ell_1 \ell_2} = -C_P^{\ell_1 \ell_2}$. For the $C_9^{\ell_1 \ell_2} - C_{10}^{\ell_1 \ell_2}$ and $C_S^{\ell_1 \ell_2} - C_P^{\ell_1 \ell_2}$ scenarios, which are independent of the charge configuration in the final state, we only consider the strongest bound in Table 3. As the interference between $C_9^{\ell_1 \ell_2}$ and $C_S^{\ell_1 \ell_2}$ depends on the charge configuration of the leptons in the final state, we present plots for both the $\tau^+ \mu^-$ and $\tau^- \mu^+$ final states. We note that the $\bar{B}_s \rightarrow \tau^- \tau^+$ decay only gives a very weak constraint in the $C_9^{\ell_1 \ell_2} = -C_{10}^{\ell_1 \ell_2}$ plane ranging from -200 to 200 . From comparison of the plots in Fig. 1, we find large differences between the $\tau^+ \mu^-$ and the $\tau^- \mu^+$. Hence, we stress that it is important to analyse these final states separately. For the electron, the differences between $\mu^- e^+$ and $\mu^+ e^-$ are negligible and we only present one figure.

As the mesonic $B^+ \rightarrow K^+ \ell_1 \ell_2$ and $\bar{B}_s \rightarrow \ell_1 \ell_2$ are mediated by the same quark level transition, we can use the obtained upper limits on combinations of Wilson coefficients and convert those into upper limit on the branching ratio and forward-backward asymmetry for $\Lambda_b \rightarrow \Lambda \ell_1 \ell_2$ decays using Eq. (15). When allowing for only one NP Wilson coefficient to be nonzero at a time, for example allowing only $C_9^{\ell_1 \ell_2} \neq 0$, the corresponding bounds can be easily obtained by calculating the scale factor between $c_{\ell_1 \ell_2}^i$ of the meson $B \rightarrow K$ LFV decay and $\xi_i^{\ell_1 \ell_2}$ of the baryon $\Lambda_b \rightarrow \Lambda$ decay using Table 1 and Table 4 and re-scaling the upper

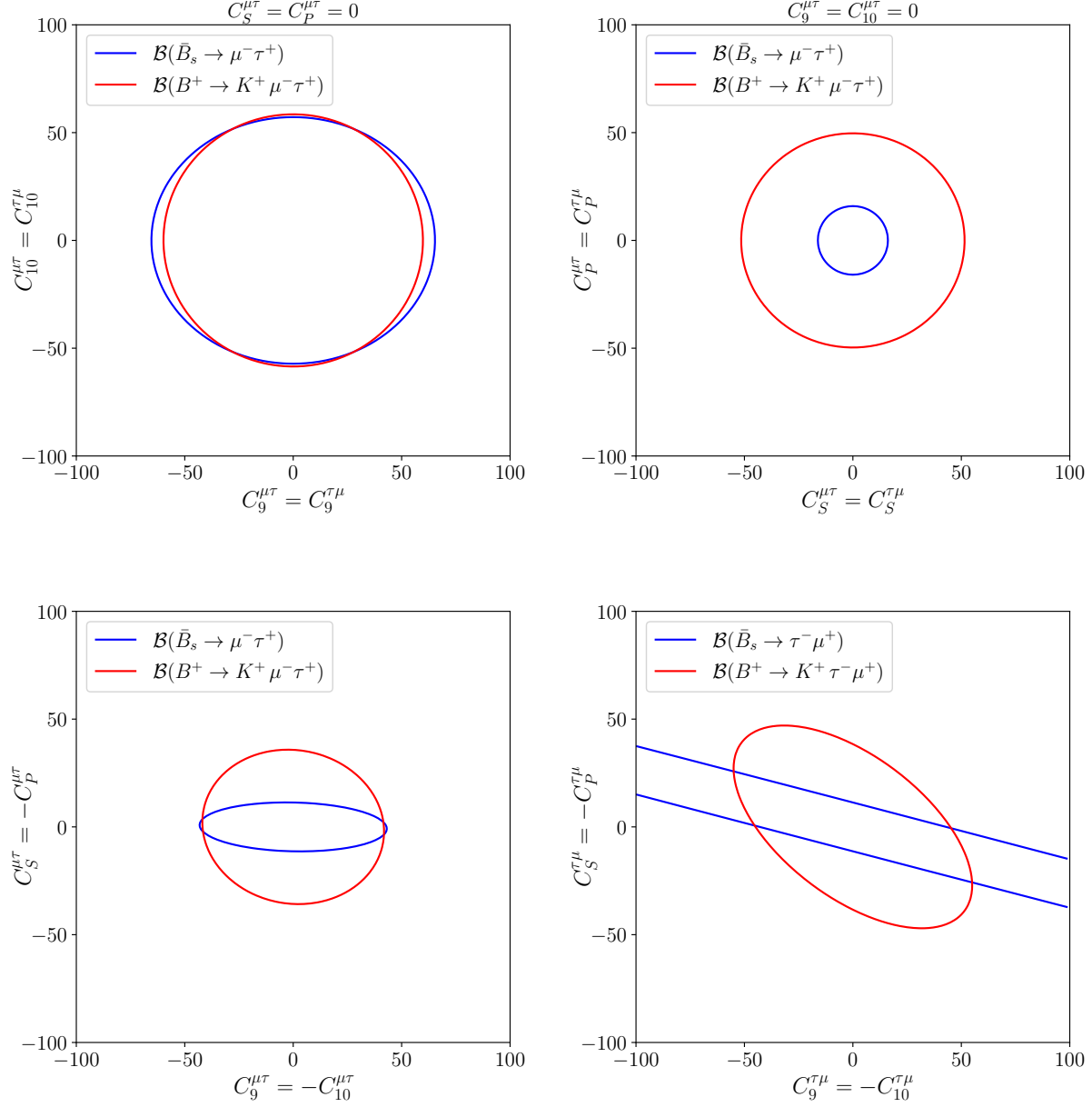


Figure 1: Model independent constraints on different combinations of Wilson coefficients obtained from the 90% C.L. upper limits on meson $b \rightarrow s\mu^\pm\tau^\mp$ transitions.

limit of the mesonic decay accordingly. In addition, comparing the coefficients in these Tables, we observe that the ratios $c_{\ell_1\ell_2}^i/c_{\ell_1\ell_2}^j$ and $\xi_i^{\ell_1\ell_2}/\xi_j^{\ell_1\ell_2}$ are very similar for $i, j = 9, 10$ and $i, j = S, P$. Therefore, the sensitivities for LFV $B \rightarrow K$ and $\Lambda_b \rightarrow \Lambda$ decays are rather similar when considering the $C_9^{\ell_1\ell_2} - C_{10}^{\ell_1\ell_2}$ only and $C_S^{\ell_1\ell_2} - C_P^{\ell_1\ell_2}$ only scenarios. Upper limits (at 90% C.L.) for the branching ratio of $\Lambda_b \rightarrow \Lambda\ell_1\ell_2$ derived from their mesonic counter

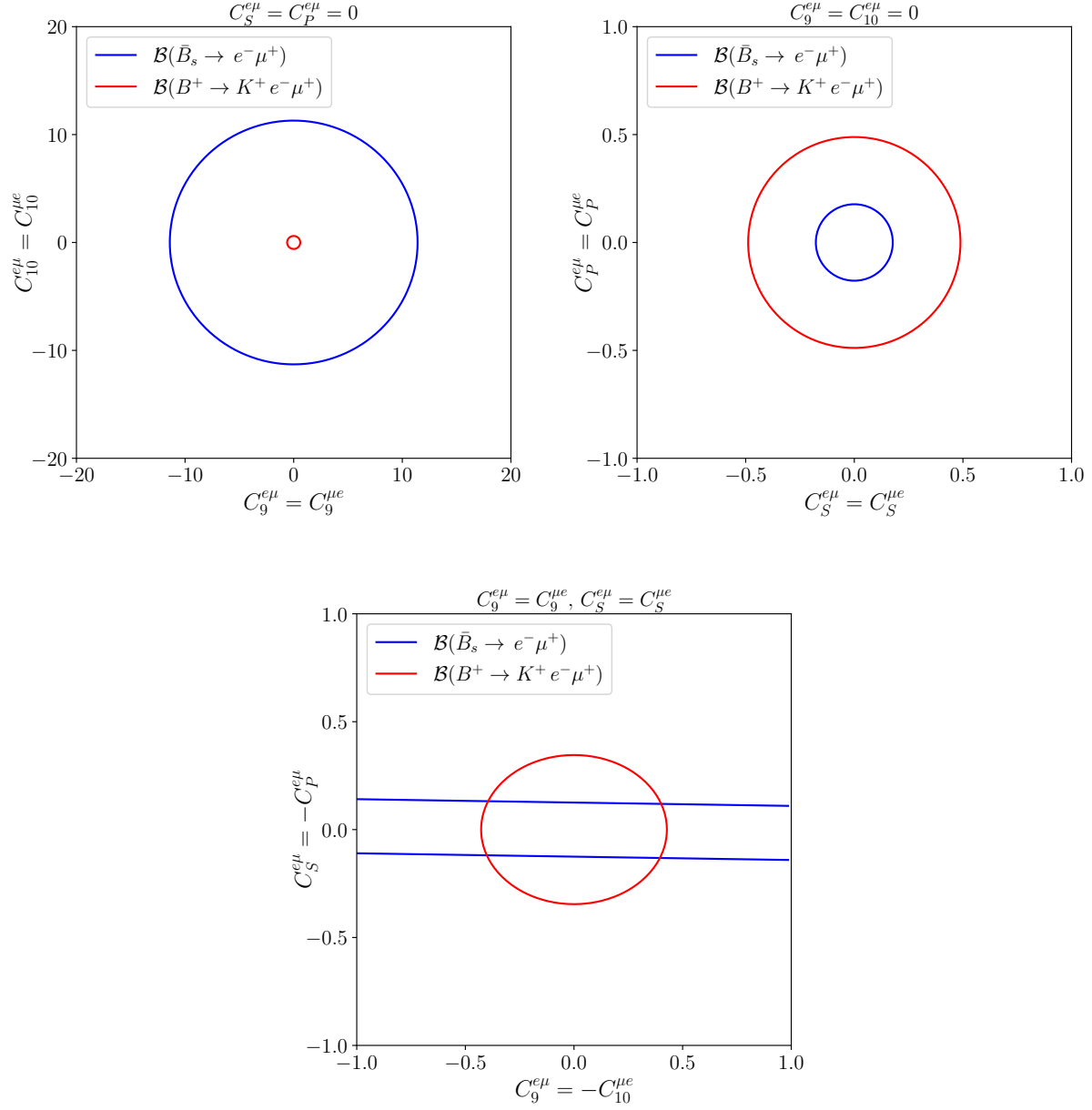


Figure 2: Model independent constraints on different combinations of Wilson coefficients obtained from the 90% C.L. upper limits on meson $b \rightarrow s\mu^\pm e^\mp$ transitions.

parts for the three scenarios are presented in Table 5. These values should be interpreted as follows: any future experimental upper limit on the baryonic mode below the quoted value gives stronger constraints on the Wilson coefficients than those obtained from the current mesonic upper limits.

The complementarity of the mesonic and the baryonic LFV channels specifically arises

	$\mathcal{B}^{\mu\tau} (\mathcal{B}^{\tau\mu}) \times 10^{-5}$	$\mathcal{B}^{e\mu} = \mathcal{B}^{\mu e} \times 10^{-8}$
$C_9^{\ell_1\ell_2} \neq 0, C_{10}^{\ell_1\ell_2} \neq 0, C_S^{\ell_1\ell_2} = C_P^{\ell_1\ell_2} = 0$	< 7.7 (7.7)	< 1.1
$C_S^{\ell_1\ell_2} \neq 0, C_P^{\ell_1\ell_2} \neq 0, C_9^{\ell_1\ell_2} = C_{10}^{\ell_1\ell_2} = 0$	< 2.7 (2.7)	< 0.06
$C_9^{\ell_1\ell_2} = -C_{10}^{\ell_1\ell_2}, C_S^{\ell_1\ell_2} = -C_P^{\ell_1\ell_2}$	< 7.4 (11)	< 1.1

Table 5: Upper limits for the branching ratio of $\Lambda_b \rightarrow \Lambda$ LFV decays obtained in a model independent way by considering their mesonic counter parts. Bounds are at 90% C.L.. For the first two scenarios, the branching ratios are independent of the charge configuration. However for the SMEFT scenario this is not the case anymore, hence we present both branching ratios for $\mu^- \tau^+$ and in brackets $\tau^- \mu^+$.

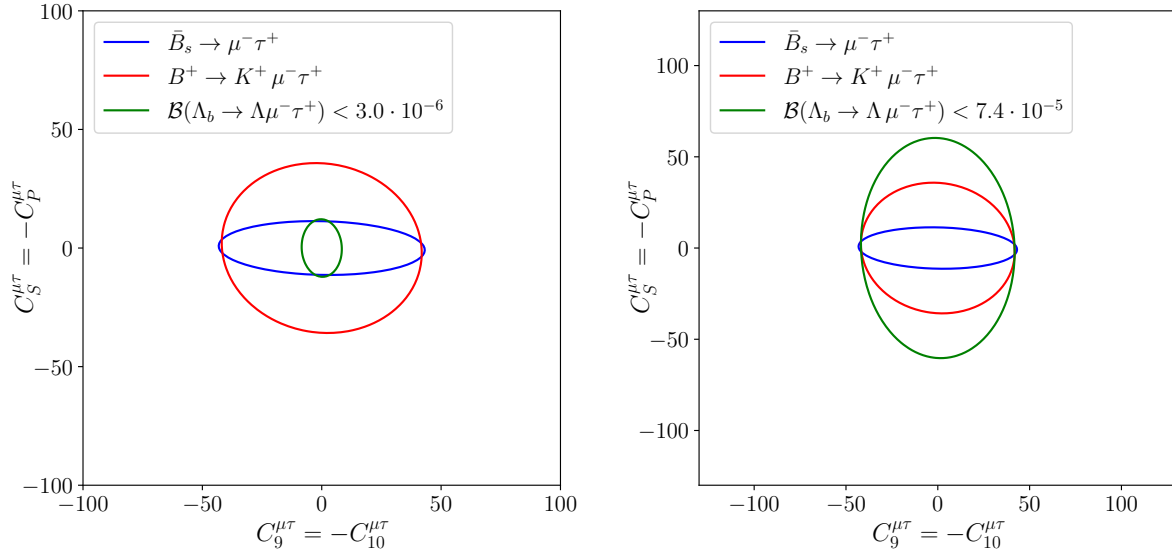


Figure 3: Illustration of the orthogonality between current mesonic and possible future baryonic constraints.

when considering both (axial)vector and (pseudo)scalar operators. We illustrate this in Fig. 3 for the SMEFT scenario where $C_9^{\ell_1\ell_2} = -C_{10}^{\ell_1\ell_2}, C_S^{\ell_1\ell_2} = -C_P^{\ell_1\ell_2}$. We present the current meson constraints combined with two possible constraints on the $\Lambda_b \rightarrow \Lambda \mu^- \tau^+$ branching ratio and observe that the mesonic modes place strong constraints on scalar/pseudoscalar interactions while the baryonic channel is more sensitive to $C_9^{\mu\tau}$ and $C_{10}^{\mu\tau}$.

Finally, we consider the integrated forward-backward asymmetry $A_{\text{FB}}^{\ell_1\ell_2}$ which provides orthogonal information compared to the branching ratio. From Eq. (15) we note the following properties: $A_{\text{FB}}^{\ell_1\ell_2}$ is identically zero if $C_9^{\ell_1\ell_2} = C_{10}^{\ell_1\ell_2} = 0$, and in the case in which only $C_9^{\ell_1\ell_2} = -C_{10}^{\ell_1\ell_2} \neq 0$ $A_{\text{FB}}^{\ell_1\ell_2}$ is independent on the values of $C_9^{\ell_1\ell_2}$ and $C_{10}^{\ell_1\ell_2}$. In the latter

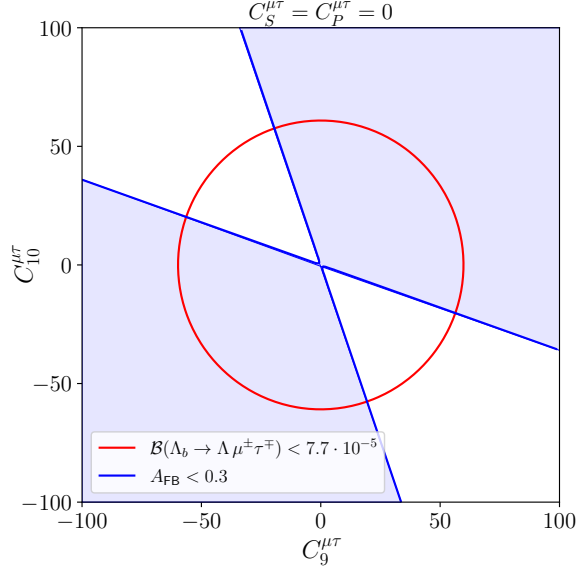


Figure 4: Illustration of how the forward-backward asymmetry provides orthogonal constraints to the branching ratio of $\Lambda_b \rightarrow \Lambda \mu^- \tau^+$. The shaded area present the allowed region for an upper limit $A_{\text{FB}}^{\mu\tau} < 0.3$, compared to an upper limit for the branching ratio of $7.7 \cdot 10^{-5}$.

scenario, we find for $C_9^{\ell_1 \ell_2} = -C_{10}^{\ell_1 \ell_2}$ and $C_S^{\ell_1 \ell_2} = C_P^{\ell_1 \ell_2} = 0$

$$A_{\text{FB}}^{\tau\mu} = 0.14 \pm 0.01, \quad A_{\text{FB}}^{\mu\tau} = 0.40 \pm 0.03, \quad A_{\text{FB}}^{e\mu} = A_{\text{FB}}^{\mu e} = 0.33 \pm 0.04. \quad (20)$$

A measurement or an upper limit different from these values provides interesting complementary information. This is illustrated in Fig. 4, where we consider for the $\mu^- \tau^+$ final state a future scenario in which an upper limit of $A_{\text{FB}}^{\mu\tau} < 0.3$ and $\mathcal{B}^{\mu\tau} < 7.7 \cdot 10^{-5}$ are considered. As we can see from Fig. 4, the information on $A_{\text{FB}}^{\tau\mu}$ helps to rule out a large part of the allowed space in the $C_9^{\ell_1 \ell_2} - C_{10}^{\ell_1 \ell_2}$ plane.

3.2 Explicit models

As mentioned, in many models that explain LFU violation, also LFV naturally occurs. Since our aim is not to perform a detailed analysis of all the observables in low-energy phenomenology, we choose to focus here on two specific models that explain the B anomalies. We choose two interesting solutions, which are the most favourite in the literature: the combination of the scalar leptoquarks S_1 and S_3 and the vector leptoquark U_1 . For these models we provide predictions for observables in $\Lambda_b \rightarrow \Lambda \ell_1^- \ell_2^+$ decays.

The $S_1 + S_3$ scalar leptoquarks scenario [42]

Here we focus on the $S_1 + S_3$ scenario, following the analysis in Ref. [42]¹. The main idea there is to apply the Froggatt-Nielsen mechanism [90], that explains the hierarchies of quark masses, as a power counting for NP operators, and thereby providing simultaneously an explanation for the B -anomalies and the flavour puzzle. Converting the formalism of Ref. [42] to the Wilson coefficients defined in Eq. (1), we find:

$$C_9^{\ell_1 \ell_2} = -C_{10}^{\ell_1 \ell_2} = \frac{v^2}{M^2} \frac{\pi}{\alpha_{\text{em}} |V_{tb} V_{ts}^*|} |g_3|^2 \tilde{S}_{QL}^{3\ell_2} \tilde{S}_{QL}^{*2\ell_1} \quad (21)$$

where M is the mass of the heavy scalar leptoquarks, $\tilde{S}_{QL}^{i\ell_i}$ is the spurion associated with the S_3 scalar leptoquark and encodes the Froggatt-Nielsen power counting, and g_3 is an overall coupling which is expected to be of $\mathcal{O}(1)$. Notice that the scalar leptoquark S_1 does not contribute to $b \rightarrow s \ell_1^- \ell_2^+$ transitions. With this, we find

$$\begin{aligned} C_9^{\mu\tau} &= -C_{10}^{\mu\tau} = -(0.41 \pm 0.07), \\ C_9^{\tau\mu} &= -C_{10}^{\tau\mu} = (10 \pm 2). \end{aligned} \quad (22)$$

For the modes with electrons and muons in the final states, we find $C_9^{e\mu} \propto 10^{-3}$ and a even lower value for $C_9^{\mu e}$. Therefore, we conclude that the corresponding branching ratios are too small to be measured by any experiment in the near future.

Focusing then on the final states with muons and taus, using the Wilson coefficients in (22) and our results in Sect. 2 gives

$$\begin{aligned} \mathcal{B}^{\mu\tau} &= (7.1 \pm 2.5) \cdot 10^{-9}, \\ \mathcal{B}^{\tau\mu} &= (4.2 \pm 1.7) \cdot 10^{-6}, \end{aligned} \quad (23)$$

where the errors are dominated by the ones on the NP Wilson coefficients. Note that since this model predicts $C_9^{\ell_1 \ell_2} = -C_{10}^{\ell_1 \ell_2}$, $A_{\text{FB}}^{\ell_1 \ell_2}$ is independent from any Wilson coefficients and assumes the value in Eq. (20). From Fig. 4 we can conclude that the $C_9^{\ell_1 \ell_2} = -C_{10}^{\ell_1 \ell_2}$ scenario would be excluded by the measurement of $A_{\text{FB}}^{\ell_1 \ell_2}$. Hence, this stresses the importance of obtaining experimental constraints on this observable.

The U_1 vector leptoquark scenario [43]

Other interesting NP models are those with a vector leptoquark, usually denoted U_1 . In fact, this NP particle is the only one able to accommodate both classes of B anomalies on its own. Among the various possibilities available in the literature, we focus on [43], where the vector leptoquark is a massive state originating from the Spontaneous Symmetry Breaking of a gauge groupe larger than the SM one. As a consequence of the gauge representation of the U_1 vector leptoquark, not only vector and axial vector couplings, but also scalar and pseudoscalar couplings are generated. In particular, the latter are very useful in explaining the large discrepancies in $b \rightarrow c \tau \bar{\nu}$ data and as a consequence, generate sizeable $b \rightarrow s \ell_1 \ell_2$

¹The analysis Ref. [42] provides qualitatively the same results as Ref. [38].

interactions. Therefore, we expect very different signatures for the U_1 model than the ones in the scalar leptoquark case. In Ref. [43] several cases are taken into account, where the flavour structure of the NP couplings has a $U(2)^5$ flavour symmetry [91] or not, and where (pseudo-)scalar couplings are present or not. In the following we report results for the case in which no $U(2)^5$ flavour symmetry is assumed. We note that using the scenario based on the $U(2)^5$ flavour symmetry yields very similar results. We also note that given the flavour structure assumed in Ref. [43], the couplings of the vector leptoquark to electrons is zero, hence no effect is predicted for $\Lambda_b \rightarrow \Lambda e^\pm \mu^\mp$. In the notation of Ref. [43] we have

$$\begin{aligned} C_9^{\ell_1 \ell_2} &= -C_{10}^{\ell_1 \ell_2} = + \frac{2\pi}{\alpha_{\text{em}} |V_{tb} V_{ts}^*|} C_U \beta_L^{2\ell_1} (\beta_L^{3\ell_2})^*, \\ C_S^{\ell_1 \ell_2} &= -C_P^{\ell_1 \ell_2} = + \frac{4\pi}{\alpha_{\text{em}} |V_{tb} V_{ts}^*|} C_U \beta_L^{2\ell_1} (\beta_R^{3\ell_2})^*, \end{aligned} \quad (24)$$

where C_U is a normalisation constant which contains the mass of the vector leptoquark normalised to the electroweak vacuum-expectation value and the gauge coupling of the leptoquark. The factor $\beta_{L(R)}^{j\beta}$ represents the coupling in flavour space to left(right)-handed fermions. In the following we neglect the uncertainties on the fitted parameters obtained from [43] due to their large and asymmetric distributions. Either way, this scenario provides a useful benchmark that allows us to predict the size of LFV $\Lambda_b \rightarrow \Lambda$ decays. We first look at the case $\beta_R^{3\beta} = 0$. We find

$$\begin{aligned} C_9^{\tau\mu} &= -C_{10}^{\tau\mu} = -5.93, \\ C_9^{\mu\tau} &= -C_{10}^{\mu\tau} = +2.90. \end{aligned} \quad (25)$$

The predictions for $A_{\text{FB}}^{\ell_1 \ell_2}$ in this case are the same as in Eq. (20). The corresponding integrated branching ratios are:

$$\begin{aligned} \mathcal{B}^{\tau\mu} &= 1.5 \times 10^{-6} \\ \mathcal{B}^{\mu\tau} &= 3.6 \times 10^{-7}. \end{aligned} \quad (26)$$

In the case where $\beta_R^{3\beta} \neq 0$, we find

$$\begin{aligned} C_9^{\tau\mu} &= -C_{10}^{\tau\mu} = -4.47, \quad C_S^{\tau\mu} = -C_P^{\tau\mu} = 0, \\ C_9^{\mu\tau} &= -C_{10}^{\mu\tau} = 2.03, \quad C_S^{\mu\tau} = -C_P^{\mu\tau} = 4.06, \end{aligned} \quad (27)$$

which yields

$$\begin{aligned} \mathcal{B}^{\tau\mu} &= 8.5 \times 10^{-7} \quad \text{and} \quad A_{\text{FB}}^{\tau\mu} = 0.14, \\ \mathcal{B}^{\mu\tau} &= 5.3 \times 10^{-7} \quad \text{and} \quad A_{\text{FB}}^{\mu\tau} = 0.12. \end{aligned} \quad (28)$$

Some comments are in order. In the scenario where $C_{S(P)}^{\ell_1 \ell_2} = 0$, $A_{\text{FB}}^{\ell_1 \ell_2}$ is independent from the Wilson coefficients and its value is given in Eq. (20). We find that $\mathcal{B}^{\tau\mu} > \mathcal{B}^{\mu\tau}$ due to a factor of two between the respective NP couplings. In the case where we have also $C_S^{\mu\tau} = -C_P^{\mu\tau} \neq 0$, we find that $\mathcal{B}^{\mu\tau}$ is surprisingly small due to the negative interference between $C_S^{\mu\tau}$ and $C_P^{\mu\tau}$. On the other hand, $A_{\text{FB}}^{\mu\tau}$ is found to be smaller than $A_{\text{FB}}^{\tau\mu}$, hence providing a possible way to distinguish the different scenarios.

3.3 LHCb prospects

The results found in the above Sections indicate that $\Lambda_b \rightarrow \Lambda \ell_1 \ell_2$ decays are very good probes of physics beyond the SM and provide in certain scenarios complementary bounds with respect to the ones from $\bar{B} \rightarrow \ell_1 \ell_2$ and $B^+ \rightarrow K^+ \ell_1 \ell_2$ decays. Here we want to comment on the prospective for measurement of $\Lambda_b \rightarrow \Lambda \ell_1 \ell_2$ decays at the LHCb experiment. If we consider measurement carried out with the same dataset, we expect for the measured yields:

$$\frac{\mathcal{N}(\Lambda_b \rightarrow \Lambda(\rightarrow p\pi)\ell_1\ell_2)}{\mathcal{N}(B^+ \rightarrow K^+\ell_1\ell_2)} = \frac{\mathcal{B}(\Lambda_b \rightarrow \Lambda(\rightarrow p\pi)\ell_1\ell_2)|_{\text{theory}}}{\mathcal{B}(B^+ \rightarrow K^+\ell_1\ell_2)|_{\text{theory}}} \frac{f_{\Lambda_b}}{f_{B^+}} r_{\Lambda_b/B^+}, \quad (29)$$

where f_{Λ_b}/f_{B^+} is the ratios of the fragmentation functions for the Λ_b and the B^+ modes, respectively, and r_{Λ_b/B^+} is a correction factor due to different reconstruction efficiencies. In Ref. [92], the ratio $f_{\Lambda_b}/(f_u + f_d)$ is measured. Using isospin relations, we can write $f_{\Lambda_b}/f_{B^+} = 2f_{\Lambda_b}/(f_u + f_d) = (0.518 \pm 0.036)$. The ratio of the predicted values of the theoretical branching ratios depends on the NP model and final state leptons. However, as we noted already in Sect. 3.1, the branching ratios for the baryon and the meson case are very similar in size: therefore, for an order of magnitude estimate, we consider them to be equal. The last piece of information needed is the ratio r_{Λ_b/B^+} , that is difficult to estimate without a thorough simulation of the LHCb detector. However, in order to give an estimate, we use the information in Refs. [6, 93], that are based on the same integrated luminosity. From these papers we extract

$$\frac{\mathcal{N}(\Lambda_b \rightarrow \Lambda(\rightarrow p\pi)\mu^-\mu^+)}{\mathcal{N}(B^+ \rightarrow K^+\mu^-\mu^+)} \approx 0.31. \quad (30)$$

This means that we expect the efficiency for the reconstruction of the Λ_b to be roughly 1.67 times less than that of the B^+ , when also taking into account the fragmentation fractions effect. Hence we set $r_{\Lambda_b/B^+} = 1.67$. We expect that all the other correction factors due to the reconstruction of the leptons in the final state cancel out since we are comparing the same leptonic final states in both decays. This yields

$$\mathcal{B}(\Lambda_b \rightarrow \Lambda(\rightarrow p\pi)\ell_1\ell_2) \approx 1.67 \frac{f_{\Lambda_b}}{f_{B^+}} \mathcal{B}(B^+ \rightarrow K^+\ell_1\ell_2). \quad (31)$$

Using the current upper limit on $\mathcal{B}(B^+ \rightarrow K^+\tau^+\mu^-)$, we thus expect that LHCb can reach the following sensitivity:

$$\mathcal{B}(\Lambda_b \rightarrow \Lambda(\rightarrow p\pi)\mu^-\tau^+) \lesssim 6.5 \cdot 10^{-5}, \quad (32)$$

for Run 1 and 2 datasets. In the above estimate, we have not included any correction for the trigger efficiency, which can be different for the baryonic and mesonic mode. The estimate in Eq. (32) can be compared to the model dependent and model independent bounds on $\mathcal{B}(\Lambda_b \rightarrow \Lambda\tau^+\mu^-)$ found in the previous Sections. In particular, the expected upper bound from LHCb would already give better constraints than the corresponding ones from the mesonic decays, as illustrated in Fig. 3. We also stress that future runs will improve the upper limit in Eq. (32) of at least a factor of roughly two with Run 3 and a factor of three with further runs [63].

4 Conclusions

In this paper, we present the first full analysis of $\Lambda_b \rightarrow \Lambda \ell_1^- \ell_2^+$ lepton flavour violating (LFV) decays in terms of possible new physics operators. The main results of this paper are Eqs. (9)–(11), where the coefficients of the angular distributions for $\Lambda_b \rightarrow \Lambda \ell_1^- \ell_2^+$ decays are given. We study the interplay between the baryonic and mesonic searches for LFV, where for the latter upper limits are already available. We convert these upper limits into constraints on the branching ratio and forward-back asymmetry for $\Lambda_b \rightarrow \Lambda \ell_1^- \ell_2^+$ decays. We find that the $\Lambda_b \rightarrow \Lambda \ell_1^- \ell_2^+$ decays provide different constraints on the new physics Wilson coefficients than $\bar{B}_s \rightarrow \ell_1^- \ell_2^+$ and $B^+ \rightarrow K^+ \ell_1^- \ell_2^+$ decays, and have the potential to reduce the allowed parameter space for new physics models. We then analyse quantitatively the size of $\Lambda_b \rightarrow \Lambda \ell_1^- \ell_2^+$ decays in specific scenarios that can address B anomalies, using as a reference [42] and [43]. Our findings indicate that the predicted branching ratio for $\Lambda_b \rightarrow \Lambda \ell_1^- \ell_2^+$ for these scenarios are such that they can further constrain the new physics couplings. As a final prospective, we estimate the reach of LHCb for $\Lambda_b \rightarrow \Lambda \ell_1^- \ell_2^+$ decays, finding that an upper limit of $\mathcal{B}(\Lambda_b \rightarrow \Lambda \mu^- \tau^+) \lesssim 6.5 \cdot 10^{-5}$ can be reached with Run 1 and Run 2 data.

Acknowledgements

We thank Yasmine Amhis, Flavio Archilli, Lex Greeven and Mick Mulder for insightful discussion on experimental prospects. The work of MB is supported by the Italian Ministry of Research (MIUR) under grant PRIN 20172LNEEZ. The work of MR is supported by the Deutsche Forschungsgemeinschaft (DFG, German Research Foundation) under grant 396021762 - TRR 257.

A Details on kinematics

In the Λ_b rest frame (Λ_b – RF), the momenta are defined as

$$q^\mu|_{\Lambda_b\text{--RF}} = (q^0, 0, 0, -|\vec{q}|), \quad (33)$$

$$k^\mu|_{\Lambda_b\text{--RF}} = (m_{\Lambda_b} - q^0, 0, 0, |\vec{q}|). \quad (34)$$

where

$$q^0|_{\Lambda_b\text{--RF}} = \frac{m_{\Lambda_b}^2 - m_\Lambda^2 + q^2}{2m_{\Lambda_b}}, \quad \text{and} \quad |\vec{q}|_{\Lambda_b\text{--RF}} = \frac{\sqrt{\lambda(m_{\Lambda_b}^2, m_\Lambda^2, q^2)}}{2m_{\Lambda_b}}, \quad (35)$$

where λ is the usual Källén function defined as $\lambda(a, b, c) = a^2 + b^2 + c^2 - 2a(b + c) - 2bc$. In the dilepton rest frame we have that $q^\mu|_{2\ell\text{--RF}} = \sqrt{q^2}(1, 0, 0, 0)$, and

$$p_1^\mu|_{2\ell\text{--RF}} = (E_{\ell_1}, -|\vec{p}_2||_{2\ell\text{--RF}} \sin \theta_\ell, 0, -|\vec{p}_2||_{2\ell\text{--RF}} \cos \theta_\ell), \quad (36)$$

$$p_2^\mu|_{2\ell\text{--RF}} = (E_{\ell_2}, +|\vec{p}_2||_{2\ell\text{--RF}} \sin \theta_\ell, 0, +|\vec{p}_2||_{2\ell\text{--RF}} \cos \theta_\ell), \quad (37)$$

where

$$|\vec{p}_2|_{|2\ell\text{-RF}} = \frac{\sqrt{\lambda(q^2, m_{\ell_1}^2, m_{\ell_2}^2)}}{2\sqrt{q^2}}, \quad \text{and} \quad E_{\ell_{1,2}} = \frac{q^2 + m_{\ell_{1,2}}^2 - m_{\ell_{2,1}}^2}{2\sqrt{q^2}}. \quad (38)$$

The two reference systems are connected by the following relation for any vector:

$$x^\mu|_{|\Lambda_b\text{-RF}} = \Lambda_{\mu\nu} x^{T\nu}, \quad \Lambda = \begin{pmatrix} \gamma & 0 & 0 & -\beta\gamma \\ 0 & 1 & 0 & 0 \\ 0 & 0 & 1 & 0 \\ -\beta\gamma & 0 & 0 & \gamma \end{pmatrix} \quad (39)$$

where $\Lambda_{\mu\nu}$ is a Lorentz transformation along the z axis. It's parameters are:

$$\gamma = \frac{q^0|_{\Lambda_b\text{-RF}}}{\sqrt{q^2}}, \quad \text{and} \quad \beta = \frac{|\vec{q}|_{|\Lambda_b\text{-RF}}}{q^0|_{\Lambda_b\text{-RF}}} \quad (40)$$

B Correlations

We present correlation matrices for the set of coefficients $\{\xi_i^{\ell_1\ell_2}, \rho_i^{\ell_1\ell_2}\}$, with the same ordering as in Tables 1–2. In Table 6 we present the correlations for μe final states and in Table 7 the ones for $\mu\tau$ final states.

1	1	0.617	0.617	0.643	0.643	-0.728	0.820	-0.839	-0.839
1	1	0.617	0.617	0.643	0.643	-0.728	0.820	-0.839	-0.839
0.617	0.617	1	1	0.885	0.885	-0.559	0.451	-0.778	-0.778
0.617	0.617	1	1	0.885	0.885	-0.559	0.451	-0.778	-0.778
0.643	0.643	0.885	0.885	1	1	-0.835	0.438	-0.911	-0.911
0.643	0.643	0.885	0.885	1	1	-0.835	0.437	-0.911	-0.911
-0.728	-0.728	-0.559	-0.559	-0.835	-0.835	1	-0.434	0.932	0.932
0.820	0.820	0.451	0.451	0.438	0.438	-0.434	1	-0.517	-0.517
-0.839	-0.839	-0.778	-0.778	-0.911	-0.911	0.932	-0.517	1	1
-0.839	-0.839	-0.778	-0.778	-0.911	-0.911	0.932	-0.517	1	1

Table 6: Correlation matrix for the $\Lambda_b \rightarrow \Lambda\mu^- e^+$ parameters.

1	0.997	0.709	0.716	-0.742	0.742	0.835	0.857	-0.877	0.877
0.997	1	0.747	0.755	-0.787	0.788	0.858	0.838	-0.900	0.900
0.709	0.747	1.00	0.999	-0.962	0.947	0.715	0.466	-0.835	0.835
0.716	0.755	0.999	1	-0.971	0.958	0.734	0.470	-0.846	0.846
-0.742	-0.787	-0.962	-0.971	1	-0.999	-0.841	-0.481	0.899	-0.899
0.742	0.788	0.947	0.958	-0.999	1	0.857	0.480	-0.903	0.903
0.835	0.858	0.715	0.734	-0.841	0.857	1	0.519	-0.964	0.964
0.857	0.838	0.466	0.470	-0.481	0.480	0.519	1	-0.544	0.544
-0.877	-0.900	-0.835	-0.846	0.899	-0.903	-0.964	-0.544	1	-1
0.877	0.900	0.835	0.846	-0.899	0.903	0.964	0.544	-1	1

Table 7: Correlation matrix for the $\Lambda_b \rightarrow \Lambda \mu^- \tau^+$ parameters.

References

- [1] LHCb collaboration, R. Aaij et al., *Test of lepton universality in beauty-quark decays*, 2103.11769.
- [2] LHCb collaboration, R. Aaij et al., *Angular Analysis of the $B^+ \rightarrow K^{*+} \mu^+ \mu^-$ Decay*, *Phys. Rev. Lett.* **126** (2021) 161802, [2012.13241].
- [3] LHCb collaboration, R. Aaij et al., *Measurement of CP-Averaged Observables in the $B^0 \rightarrow K^{*0} \mu^+ \mu^-$ Decay*, *Phys. Rev. Lett.* **125** (2020) 011802, [2003.04831].
- [4] LHCb collaboration, R. Aaij et al., *Test of lepton universality using $B^+ \rightarrow K^+ \ell^+ \ell^-$ decays*, *Phys. Rev. Lett.* **113** (2014) 151601, [1406.6482].
- [5] LHCb collaboration, R. Aaij et al., *Test of lepton universality with $B^0 \rightarrow K^{*0} \ell^+ \ell^-$ decays*, *JHEP* **08** (2017) 055, [1705.05802].
- [6] LHCb collaboration, R. Aaij et al., *Search for lepton-universality violation in $B^+ \rightarrow K^+ \ell^+ \ell^-$ decays*, *Phys. Rev. Lett.* **122** (2019) 191801, [1903.09252].
- [7] LHCb collaboration, R. Aaij et al., *Angular analysis of the $B^0 \rightarrow K^{*0} \mu^+ \mu^-$ decay using 3 fb^{-1} of integrated luminosity*, *JHEP* **02** (2016) 104, [1512.04442].
- [8] BABAR collaboration, J. P. Lees et al., *Evidence for an excess of $\bar{B} \rightarrow D^{(*)} \tau^- \bar{\nu}_\tau$ decays*, *Phys. Rev. Lett.* **109** (2012) 101802, [1205.5442].
- [9] BABAR collaboration, J. P. Lees et al., *Measurement of an Excess of $\bar{B} \rightarrow D^{(*)} \tau^- \bar{\nu}_\tau$ Decays and Implications for Charged Higgs Bosons*, *Phys. Rev. D* **88** (2013) 072012, [1303.0571].

- [10] LHCb collaboration, R. Aaij et al., *Measurement of the ratio of branching fractions $\mathcal{B}(\bar{B}^0 \rightarrow D^{*+}\tau^-\bar{\nu}_\tau)/\mathcal{B}(\bar{B}^0 \rightarrow D^{*+}\mu^-\bar{\nu}_\mu)$* , *Phys. Rev. Lett.* **115** (2015) 111803, [1506.08614].
- [11] BELLE collaboration, S. Hirose et al., *Measurement of the τ lepton polarization and $R(D^*)$ in the decay $\bar{B} \rightarrow D^*\tau^-\bar{\nu}_\tau$* , *Phys. Rev. Lett.* **118** (2017) 211801, [1612.00529].
- [12] BELLE collaboration, S. Hirose et al., *Measurement of the τ lepton polarization and $R(D^*)$ in the decay $\bar{B} \rightarrow D^*\tau^-\bar{\nu}_\tau$ with one-prong hadronic τ decays at Belle*, *Phys. Rev. D* **97** (2018) 012004, [1709.00129].
- [13] LHCb collaboration, R. Aaij et al., *Measurement of the ratio of the $B^0 \rightarrow D^{*-}\tau^+\nu_\tau$ and $B^0 \rightarrow D^{*-}\mu^+\nu_\mu$ branching fractions using three-prong τ -lepton decays*, *Phys. Rev. Lett.* **120** (2018) 171802, [1708.08856].
- [14] LHCb collaboration, R. Aaij et al., *Test of Lepton Flavor Universality by the measurement of the $B^0 \rightarrow D^{*-}\tau^+\nu_\tau$ branching fraction using three-prong τ decays*, *Phys. Rev. D* **97** (2018) 072013, [1711.02505].
- [15] BELLE collaboration, A. Abdesselam et al., *Measurement of $\mathcal{R}(D)$ and $\mathcal{R}(D^*)$ with a semileptonic tagging method*, 1904.08794.
- [16] L. Di Luzio, A. Greljo and M. Nardecchia, *Gauge leptoquark as the origin of B-physics anomalies*, *Phys. Rev. D* **96** (2017) 115011, [1708.08450].
- [17] L. Calibbi, A. Crivellin and T. Li, *Model of vector leptoquarks in view of the B-physics anomalies*, *Phys. Rev. D* **98** (2018) 115002, [1709.00692].
- [18] R. Barbieri and A. Tesi, *B-decay anomalies in Pati-Salam $SU(4)$* , *Eur. Phys. J. C* **78** (2018) 193, [1712.06844].
- [19] M. Blanke and A. Crivellin, *B Meson Anomalies in a Pati-Salam Model within the Randall-Sundrum Background*, *Phys. Rev. Lett.* **121** (2018) 011801, [1801.07256].
- [20] L. Di Luzio, J. Fuentes-Martin, A. Greljo, M. Nardecchia and S. Renner, *Maximal Flavour Violation: a Cabibbo mechanism for leptoquarks*, *JHEP* **11** (2018) 081, [1808.00942].
- [21] T. Faber, M. Hudec, M. Malinský, P. Meinzinger, W. Porod and F. Staub, *A unified leptoquark model confronted with lepton non-universality in B-meson decays*, *Phys. Lett. B* **787** (2018) 159–166, [1808.05511].
- [22] J. Heeck and D. Teresi, *Pati-Salam explanations of the B-meson anomalies*, *JHEP* **12** (2018) 103, [1808.07492].
- [23] A. Angelescu, D. Bečirević, D. A. Faroughy and O. Sumensari, *Closing the window on single leptoquark solutions to the B-physics anomalies*, *JHEP* **10** (2018) 183, [1808.08179].

- [24] M. Schmaltz and Y.-M. Zhong, *The leptoquark Hunter’s guide: large coupling*, *JHEP* **01** (2019) 132, [1810.10017].
- [25] A. Greljo, J. Martin Camalich and J. D. Ruiz-Álvarez, *Mono- τ Signatures at the LHC Constrain Explanations of B-decay Anomalies*, *Phys. Rev. Lett.* **122** (2019) 131803, [1811.07920].
- [26] B. Fornal, S. A. Gadam and B. Grinstein, *Left-Right $SU(4)$ Vector Leptoquark Model for Flavor Anomalies*, *Phys. Rev. D* **99** (2019) 055025, [1812.01603].
- [27] M. J. Baker, J. Fuentes-Martín, G. Isidori and M. König, *High- p_T signatures in vector-leptoquark models*, *Eur. Phys. J. C* **79** (2019) 334, [1901.10480].
- [28] C. Cornella, J. Fuentes-Martin and G. Isidori, *Revisiting the vector leptoquark explanation of the B-physics anomalies*, *JHEP* **07** (2019) 168, [1903.11517].
- [29] L. Da Rold and F. Lamagna, *A vector leptoquark for the B-physics anomalies from a composite GUT*, *JHEP* **12** (2019) 112, [1906.11666].
- [30] M. Bordone, C. Cornella, J. Fuentes-Martin and G. Isidori, *A three-site gauge model for flavor hierarchies and flavor anomalies*, *Phys. Lett. B* **779** (2018) 317–323, [1712.01368].
- [31] M. Bordone, C. Cornella, J. Fuentes-Martín and G. Isidori, *Low-energy signatures of the PS^3 model: from B-physics anomalies to LFV*, *JHEP* **10** (2018) 148, [1805.09328].
- [32] M. Bordone, O. Catà and T. Feldmann, *Effective Theory Approach to New Physics with Flavour: General Framework and a Leptoquark Example*, *JHEP* **01** (2020) 067, [1910.02641].
- [33] D. Marzocca, *Addressing the B-physics anomalies in a fundamental Composite Higgs Model*, *JHEP* **07** (2018) 121, [1803.10972].
- [34] D. Bečirević, I. Doršner, S. Fajfer, N. Košnik, D. A. Faroughy and O. Sumensari, *Scalar leptoquarks from grand unified theories to accommodate the B-physics anomalies*, *Phys. Rev. D* **98** (2018) 055003, [1806.05689].
- [35] I. Bigaran, J. Gargalionis and R. R. Volkas, *A near-minimal leptoquark model for reconciling flavour anomalies and generating radiative neutrino masses*, *JHEP* **10** (2019) 106, [1906.01870].
- [36] A. Crivellin, D. Müller and F. Saturnino, *Flavor Phenomenology of the Leptoquark Singlet-Triplet Model*, *JHEP* **06** (2020) 020, [1912.04224].
- [37] S. Saad, *Combined explanations of $(g - 2)_\mu$, $R_{D^{(*)}}$, $R_{K^{(*)}}$ anomalies in a two-loop radiative neutrino mass model*, *Phys. Rev. D* **102** (2020) 015019, [2005.04352].

- [38] V. Gherardi, D. Marzocca and E. Venturini, *Low-energy phenomenology of scalar leptoquarks at one-loop accuracy*, *JHEP* **01** (2021) 138, [2008.09548].
- [39] K. S. Babu, P. S. B. Dev, S. Jana and A. Thapa, *Unified framework for B -anomalies, muon $g - 2$ and neutrino masses*, *JHEP* **03** (2021) 179, [2009.01771].
- [40] A. Crivellin, D. Müller and T. Ota, *Simultaneous explanation of $R(D^{(*)})$ and $b \rightarrow s\mu^+\mu^-$: the last scalar leptoquarks standing*, *JHEP* **09** (2017) 040, [1703.09226].
- [41] D. Buttazzo, A. Greljo, G. Isidori and D. Marzocca, *B -physics anomalies: a guide to combined explanations*, *JHEP* **11** (2017) 044, [1706.07808].
- [42] M. Bordone, O. Catà, T. Feldmann and R. Mandal, *Constraining flavour patterns of scalar leptoquarks in the effective field theory*, *JHEP* **03** (2021) 122, [2010.03297].
- [43] C. Cornella, D. A. Faroughy, J. Fuentes-Martín, G. Isidori and M. Neubert, *Reading the footprints of the B -meson flavor anomalies*, 2103.16558.
- [44] D. Marzocca and S. Trifinopoulos, *A Minimal Explanation of Flavour Anomalies: B -Meson Decays, Muon Magnetic Moment, and the Cabbibo Angle*, 2104.05730.
- [45] A. Greljo, P. Stangl and A. E. Thomsen, *A Model of Muon Anomalies*, 2103.13991.
- [46] J. Davighi, *Anomalous Z' bosons for anomalous B decays*, 2105.06918.
- [47] J. S. Alvarado, S. F. Mantilla, R. Martinez and F. Ochoa, *A non-universal $U(1)_X$ extension to the Standard Model to study the B meson anomaly and muon $g - 2$* , 2105.04715.
- [48] P. Fileviez Pérez, C. Murgui and A. D. Plascencia, *Leptoquarks and Matter Unification: Flavor Anomalies and the Muon $g - 2$* , 2104.11229.
- [49] J.-Y. Cen, Y. Cheng, X.-G. He and J. Sun, *Flavor Specific $U(1)_{B_q-L_\mu}$ Gauge Model for Muon $g - 2$ and $b \rightarrow s\bar{\mu}\mu$ Anomalies*, 2104.05006.
- [50] J. Chen, Q. Wen, F. Xu and M. Zhang, *Flavor Anomalies Accommodated in A Flavor Gauged Two Higgs Doublet Model*, 2104.03699.
- [51] T. Nomura and H. Okada, *Explanations for anomalies of muon anomalous magnetic dipole moment, $b \rightarrow s\mu\bar{\mu}$ and radiative neutrino masses in a leptoquark model*, 2104.03248.
- [52] H. M. Lee, *Leptoquark Option for B -meson Anomalies and Leptonic Signatures*, 2104.02982.
- [53] G. Arcadi, L. Calibbi, M. Fedele and F. Mescia, *Muon $g - 2$ and B -anomalies from Dark Matter*, 2104.03228.

- [54] R. Barbieri, *A view of flavour physics in 2021*, 2103.15635.
- [55] G. Hiller, D. Loose and I. Nišandžić, *Flavorful leptoquarks at the LHC and beyond: Spin 1*, 2103.12724.
- [56] A. Angelescu, D. Bečirević, D. A. Faroughy, F. Jaffredo and O. Sumensari, *On the single leptoquark solutions to the B-physics anomalies*, 2103.12504.
- [57] J. Alda, J. Guasch and S. Peñaranda, *Anomalies in B mesons decays: A phenomenological approach*, 2012.14799.
- [58] T. Blake, S. Meinel and D. van Dyk, *Bayesian Analysis of $b \rightarrow s\mu^+\mu^-$ Wilson Coefficients using the Full Angular Distribution of $\Lambda_b \rightarrow \Lambda(\rightarrow p\pi^-)\mu^+\mu^-$ Decays*, *Phys. Rev. D* **101** (2020) 035023, [1912.05811].
- [59] M. Algueró, B. Capdevila, S. Descotes-Genon, J. Matias and M. Novoa-Brunet, *$b \rightarrow s\ell\ell$ global fits after Moriond 2021 results*, in *55th Rencontres de Moriond on Electroweak Interactions and Unified Theories*, 4, 2021. 2104.08921.
- [60] W. Altmannshofer and P. Stangl, *New Physics in Rare B Decays after Moriond 2021*, 2103.13370.
- [61] T. Hurth, F. Mahmoudi, D. M. Santos and S. Neshatpour, *More Indications for Lepton Nonuniversality in $b \rightarrow s\ell^+\ell^-$* , 2104.10058.
- [62] M. Ciuchini, A. M. Coutinho, M. Fedele, E. Franco, A. Paul, L. Silvestrini et al., *New Physics in $b \rightarrow s\ell^+\ell^-$ confronts new data on Lepton Universality*, *Eur. Phys. J. C* **79** (2019) 719, [1903.09632].
- [63] LHCb collaboration, R. Aaij et al., *Physics case for an LHCb Upgrade II - Opportunities in flavour physics, and beyond, in the HL-LHC era*, 1808.08865.
- [64] S. Sahoo and R. Mohanta, *Effects of scalar leptoquark on semileptonic Λ_b decays*, *New J. Phys.* **18** (2016) 093051, [1607.04449].
- [65] T. Feldmann and M. W. Y. Yip, *Form factors for $\Lambda_b \rightarrow \Lambda$ transitions in the soft-collinear effective theory*, *Phys. Rev. D* **85** (2012) 014035, [1111.1844].
- [66] W. Detmold and S. Meinel, *$\Lambda_b \rightarrow \Lambda\ell^+\ell^-$ form factors, differential branching fraction, and angular observables from lattice QCD with relativistic b quarks*, *Phys. Rev. D* **93** (2016) 074501, [1602.01399].
- [67] A. Datta, S. Kamali, S. Meinel and A. Rashed, *Phenomenology of $\Lambda_b \rightarrow \Lambda_c\tau\bar{\nu}_\tau$ using lattice QCD calculations*, *JHEP* **08** (2017) 131, [1702.02243].
- [68] P. Böer, T. Feldmann and D. van Dyk, *Angular Analysis of the Decay $\Lambda_b \rightarrow \Lambda(\rightarrow N\pi)\ell^+\ell^-$* , *JHEP* **01** (2015) 155, [1410.2115].

- [69] PARTICLE DATA GROUP collaboration, P. Zyla et al., *Review of Particle Physics*, *PTEP* **2020** (2020) 083C01.
- [70] K. G. Chetyrkin, J. H. Kuhn and M. Steinhauser, *RunDec: A Mathematica package for running and decoupling of the strong coupling and quark masses*, *Comput. Phys. Commun.* **133** (2000) 43–65, [[hep-ph/0004189](#)].
- [71] S. Descotes-Genon and M. Novoa-Brunet, *Angular analysis of the rare decay $\Lambda_b \rightarrow \Lambda(1520)(\rightarrow NK)\ell^+\ell^-$* , *JHEP* **06** (2019) 136, [[1903.00448](#)].
- [72] M. Bordone, *Heavy Quark Expansion of $\Lambda_b \rightarrow \Lambda^*(1520)$ Form Factors beyond Leading Order*, *Symmetry* **13** (2021) 531, [[2101.12028](#)].
- [73] D. Das and J. Das, *The $\Lambda_b \rightarrow \Lambda^*(1520)(\rightarrow N\bar{K})\ell^+\ell^-$ decay at low-recoil in HQET*, *JHEP* **07** (2020) 002, [[2003.08366](#)].
- [74] HFLAV collaboration, Y. S. Amhis et al., *Averages of b -hadron, c -hadron, and τ -lepton properties as of 2018*, *Eur. Phys. J.* **C81** (2021) 226, [[1909.12524](#)].
- [75] UTFIT collaboration. <http://www.utfit.org/UTfit/WebHome>.
- [76] B. Grzadkowski, M. Iskrzynski, M. Misiak and J. Rosiek, *Dimension-Six Terms in the Standard Model Lagrangian*, *JHEP* **10** (2010) 085, [[1008.4884](#)].
- [77] C. Bobeth, G. Hiller and G. Piranishvili, *Angular distributions of $\bar{B} \rightarrow \bar{K}\ell^+\ell^-$ decays*, *JHEP* **12** (2007) 040, [[0709.4174](#)].
- [78] G. Hiller and M. Schmaltz, *R_K and future $b \rightarrow s\ell\ell$ physics beyond the standard model opportunities*, *Phys. Rev. D* **90** (2014) 054014, [[1408.1627](#)].
- [79] LHCb collaboration, R. Aaij et al., *Search for the lepton-flavour-violating decays $B_s^0 \rightarrow \tau^\pm\mu^\mp$ and $B^0 \rightarrow \tau^\pm\mu^\mp$* , *Phys. Rev. Lett.* **123** (2019) 211801, [[1905.06614](#)].
- [80] LHCb collaboration, R. Aaij et al., *Search for the lepton-flavour violating decays $B_{(s)}^0 \rightarrow e^\pm\mu^\mp$* , *JHEP* **03** (2018) 078, [[1710.04111](#)].
- [81] BABAR collaboration, J. P. Lees et al., *A search for the decay modes $B^{+-} \rightarrow h^{+-}\tau^{+-}l$* , *Phys. Rev. D* **86** (2012) 012004, [[1204.2852](#)].
- [82] LHCb collaboration, R. Aaij et al., *Search for the lepton flavour violating decay $B^+ \rightarrow K^+\mu^-\tau^+$ using B_{s2}^{*0} decays*, *JHEP* **06** (2020) 129, [[2003.04352](#)].
- [83] LHCb collaboration, R. Aaij et al., *Search for Lepton-Flavor Violating Decays $B^+ \rightarrow K^+\mu^\pm e^\mp$* , *Phys. Rev. Lett.* **123** (2019) 241802, [[1909.01010](#)].
- [84] HPQCD collaboration, C. Bouchard, G. P. Lepage, C. Monahan, H. Na and J. Shigemitsu, *Rare decay $B \rightarrow K\ell^+\ell^-$ form factors from lattice QCD*, *Phys. Rev. D* **88** (2013) 054509, [[1306.2384](#)].

- [85] N. Gubernari, A. Kokulu and D. van Dyk, *B → P and B → V Form Factors from B-Meson Light-Cone Sum Rules beyond Leading Twist*, *JHEP* **01** (2019) 150, [1811.00983].
- [86] D. Bečirević, N. Košnik, O. Sumensari and R. Zukanovich Funchal, *Palatable Leptoquark Scenarios for Lepton Flavor Violation in Exclusive $b \rightarrow s\ell_1\ell_2$ modes*, *JHEP* **11** (2016) 035, [1608.07583].
- [87] J. Gratx, M. Hopfer and R. Zwicky, *Generalised helicity formalism, higher moments and the $B \rightarrow K_{JK}(\rightarrow K\pi)\ell_1\ell_2$ angular distributions*, *Phys. Rev. D* **93** (2016) 054008, [1506.03970].
- [88] R. Balasubramanian and B. Blossier, *Decay constant of B_s and B_s^* mesons from $N_f = 2$ lattice QCD*, *Eur. Phys. J. C* **80** (2020) 412, [1912.09937].
- [89] D. Lancierini, G. Isidori, P. Owen and N. Serra, *On the significance of new physics in $b \rightarrow s\ell^+\ell^-$ decays*, 2104.05631.
- [90] C. D. Froggatt and H. B. Nielsen, *Hierarchy of Quark Masses, Cabibbo Angles and CP Violation*, *Nucl. Phys. B* **147** (1979) 277–298.
- [91] R. Barbieri, G. Isidori, J. Jones-Perez, P. Lodone and D. M. Straub, *U(2) and Minimal Flavour Violation in Supersymmetry*, *Eur. Phys. J. C* **71** (2011) 1725, [1105.2296].
- [92] LHCb collaboration, R. Aaij et al., *Measurement of b hadron fractions in 13 TeV pp collisions*, *Phys. Rev. D* **100** (2019) 031102, [1902.06794].
- [93] LHCb collaboration, R. Aaij et al., *Angular moments of the decay $\Lambda_b^0 \rightarrow \Lambda\mu^+\mu^-$ at low hadronic recoil*, *JHEP* **09** (2018) 146, [1808.00264].